

# Telecom technology based continuous wave terahertz photomixing system with 105 decibel signal-to-noise ratio and 3.5 terahertz bandwidth

Thorsten Göbel,\* Dennis Stanze, Björn Globisch, Roman J. B. Dietz, Helmut Roehle, and Martin Schell

Fraunhofer Institute for Telecommunications, Heinrich Hertz Institute, Einsteinufer 37, 10587 Berlin, Germany

\*Corresponding author: Thorsten.Goebel@hhi.fraunhofer.de

Received July 3, 2013; revised September 11, 2013; accepted September 16, 2013;

posted September 17, 2013 (Doc. ID 193269); published October 14, 2013

A modified photoconductive receiver significantly improves the performance of photomixing-based continuous wave (cw) THz systems driven at the optical telecommunication wavelength of 1.5  $\mu\text{m}$ . The achieved signal-to-noise ratio of 105 dB at 100 GHz and 70 dB at 1 THz, both for an integration time of 200 ms, are to our knowledge the highest numbers reported in literature for any optoelectronic cw THz system, including classical setups operating at 800 nm. The developed receiver allows for combining low cost and high performance in one system for the first time to our knowledge. © 2013 Optical Society of America

OCIS codes: (300.6495) Spectroscopy, terahertz; (250.0250) Optoelectronics; (040.5150) Photoconductivity; (040.2235) Far infrared or terahertz.

<http://dx.doi.org/10.1364/OL.38.004197>

Photoconductive techniques have become a well-established way to access THz frequencies within the last years. Time domain (TD) [1] and continuous wave (cw) [2] THz systems have become mature and ready for everyday use. Nevertheless, and despite many applications having been demonstrated, the industrial breakthrough is yet to come. One candidate to fulfill the industry's demand for cost-effective and reliable systems is a photoconductive system operating at the optical communication wavelength of 1.5  $\mu\text{m}$  [3,4]. CW THz systems especially profit from telecom technologies, since the required optical components are available from stock at low price. Up to now, 1.5  $\mu\text{m}$  cw THz systems have suffered from an inferior signal-to-noise ratio (SNR) as compared to their 800 nm counterpart. Hence, the system of choice for the vast majority of THz users operated at 800 nm, despite the considerably higher component costs.

In this Letter, we present a modified photoconductive receiver which significantly improves the performance of 1.5  $\mu\text{m}$  cw THz photomixing systems. The achieved SNR is, to our knowledge, the highest value reported in the literature for any optoelectronic cw THz system. Thus, for the first time, low system cost and superior performance are unified in a single system. This development in the field of cw THz photomixing systems is a significant contribution to the breakthrough of this technology.

The attractiveness of telecom technology based photomixing systems has triggered intense research activity into suitable material systems in the past [5–7]. The most successful approach yet is a low-temperature-grown  $\text{In}_{0.53}\text{Ga}_{0.47}\text{As}/\text{In}_{0.52}\text{Al}_{0.48}\text{As}$  heterostructure [8], where the InGaAs serves as absorbing layer while the InAlAs provides deep trap states required for fast recombination and high dark resistivity. To this day, the thickness of the InGaAs (12 nm) and the InAlAs (8 nm) layers as well as the number of periods (100) has not been optimized for cw operation. As a first step toward highly efficient cw THz receivers, we varied the thickness of the InGaAs layers. The InAlAs thickness (8 nm) as well as the

number of periods (100) remained unchanged for the sake of comparison.

Increasing the InGaAs thickness for improvement of the receiver performance is motivated by absorption measurements, which revealed that only 80% of the light is absorbed by the previous design. Further, carriers generated at the same penetration depth will have to cross less InGaAs/InAlAs interfaces before getting to the contact metallization for thicker InGaAs layers. Thus, the modified device should not only absorb a larger fraction of the incident light, but also feature a higher mobility. The contact metallization (Ti/Pt/Au) of the photomixer features a standard interdigital design (see Fig. 1), with a finger separation of 1.7  $\mu\text{m}$  and a finger width of 0.3  $\mu\text{m}$  each. These dimensions are identical to the previous layout, too, since the sole influence of the InGaAs layer thickness was of interest at first. The THz receiver is completed by a 90° bow-tie antenna with 3 mm

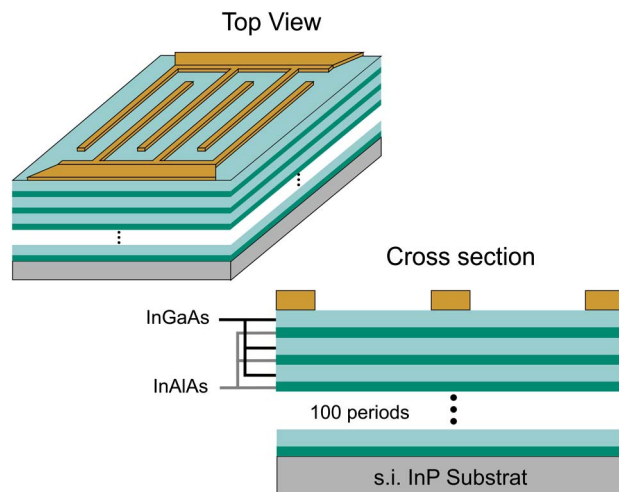


Fig. 1. Semiconductor structure and contact metallization of the photomixer. To optimize the performance as a cw THz receiver, the thickness of the InGaAs layers was increased from 12 to 24 nm in steps of 6 nm.

diameter [8], which is required for receiving the THz signal in the coherent experiment.

At first, we investigated the responsivity of the modified receiver on the chip level. Here, we defined the responsivity as ratio of generated photocurrent and applied electrical field for a specific optical illumination power. To emulate an incident THz wave, which will provide the electric field in the coherent experiment, we applied a constant bias of 0.5 V to the photoconductive chips. This (DC) responsivity was determined as a function of the optical illumination power. The results in Fig. 2 show that the responsivity strongly increases with the thickness of the InGaAs layers. For a distinct illustration of the improvement, we additionally normalized the responsivity to the maximum of the old receiver design (i.e., 12 nm InGaAs). This reveals that the responsivity shows a 6.5-fold increase for identical operation conditions if the thickness of the InGaAs layer is doubled. In the case of limited optical power ( $P_{\text{opt}} < 30$  mW), one can profit from the enhanced receiver design, too, since the responsivity of the previous receiver was obtained with a sixth of the optical power only.

While the responsivity is a linear function of the optical power for all samples within the depicted range, saturation becomes apparent for higher thickness of the InGaAs layers. The increase from 12 to 18 nm caused a 4.5-fold rise of the responsivity, whereas an additional 6 nm only resulted in a further 1.5-fold improvement. This saturation behavior is expected, since the absorption of light in a semiconductor is a mono-exponential function. The absorption coefficient of the multilayer structure was determined to be in the range of  $7000\text{--}10,000\text{ cm}^{-1}$ . Thus, 100 periods of the 12/8 nm structure capture roughly 80% of the light, while the 24/8 nm receiver is absorbing nearly 94% of the incident signal. An exponential fit to the measured values reveals that the InGaAs thickness needs to be approximately 50 nm to capture the rest of the light. This would result in a total stack height of  $5.8\text{ }\mu\text{m}$  and since molecular beam epitaxy growth becomes aggravated with the total thickness of the grown semiconductor, we forgo the realization of even thicker structures at this point. In addition, thicker InGaAs layers will decrease the resistance of the

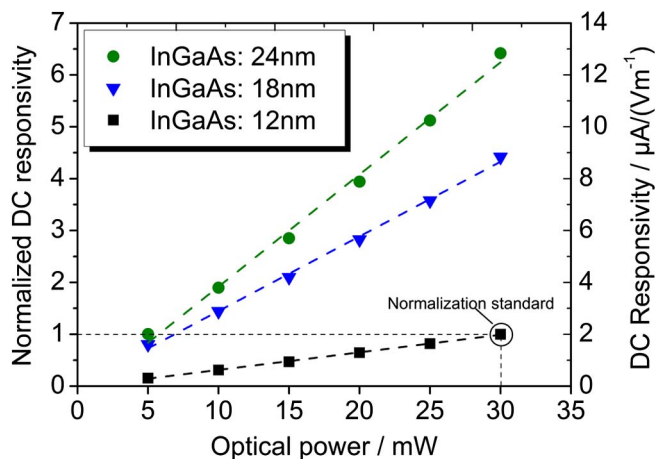


Fig. 2. DC responsivity versus optical power and InGaAs layer thickness. The symbols mark measurement points; the dashed lines are a linear fit.

photoconductor, since the trapping into the InAlAs becomes less probable, which will result in higher noise. Thus, further studies have to show which InGaAs layer thickness is the most advantageous concerning the SNR.

Next, the THz performance of the modified receiver chip was evaluated. The optical part of the coherent THz system, including the lasers, the 3 dB coupler, and the delay stage is described in [9]. For convenient handling and stability, the new receiver chips were mounted into a fiber-coupled module, which is shown as an inset in Fig. 3. An emitter serves a fast PIN photodiode [8,9] which is also mounted into a fiber-coupled module. For the measurement, the emitter was biased with  $-1.5$  V and illuminated with an optical power of 30 mW.

The corresponding THz power was determined with a calibrated Golay cell (Tydex GC-1P) and amounts to  $10\text{ }\mu\text{W}$  at 100 GHz, dropping to 100 nW at 1 THz. At the receiver, the optical power was reduced to 20 mW, since we obtained the best signal-to-noise performance at this particular value. The THz path of the setup features two  $90^\circ$  off-axis parabolic mirrors, with 2" diameter and 3" focal length, leading to a total length of the THz path of approximately 30 cm. For realization of a lock-in-amplifier, the chopping signal and the detected photocurrent were sampled synchronously with a fast 24-bit analog-to-digital-converter (ADC) (NI PXI 5922) and processed correspondingly.

The frequency range from 100 GHz to 3.6 THz was scanned in steps of 5 GHz. First, the results in Fig. 3 show that the PIN photodiode used as transmitter does emit coherent THz radiation up to 3.5 THz. This is, according to our knowledge, the highest frequency generated by a diode-based photomixing device yet. We obtained an SNR as high as 105 dB at a frequency of 100 GHz. We nearly reach 70 dB at 1 THz and 45 dB at 2 THz, all for an integration time of 200 ms. This is a 20 dB improvement as compared to previous results for  $1.5\text{ }\mu\text{m}$  systems [9] and is 12 dB superior to state-of-the-art 800 nm systems [10]. We note that the SNR was in fact limited by

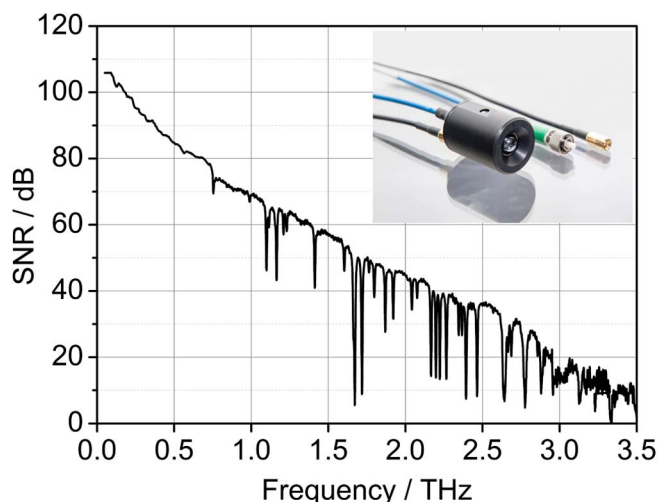


Fig. 3. SNR of the coherent THz system for the 24/8 nm InGaAs/InAlAs receiver and an integration time of 200 ms. The inset shows the fiber-coupled module, whose dimensions (25 mm diameter, 32 mm length) are identical for emitter and receiver.

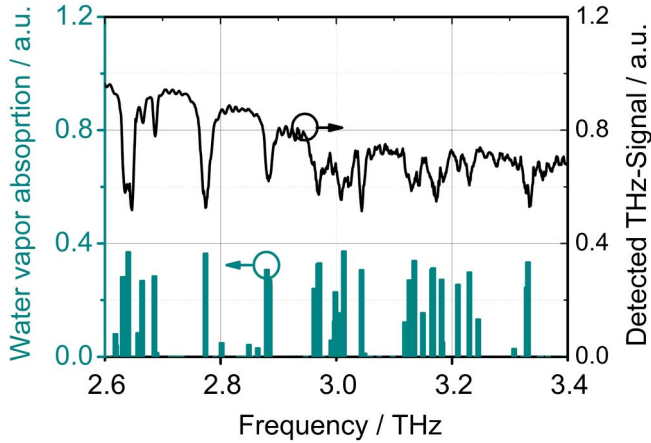


Fig. 4. Detected THz signal in comparison with the water vapor absorption lines as found in the HITRAN database for the frequency range from 2.6–3.4 THz. We note that the absorption line at 3.335 THz is clearly visible.

the dynamic range used, ADC, leading to the plateau visible around 100 GHz. The noise floor of the system was identified at 3.6 THz, which denotes a bandwidth improvement of 50% as compared to the previous semiconductor design. Figure 4 shows a comparison of the detected THz signal and the water vapor absorption lines as found in the HITRAN database. For this measurement, the frequency range from 2.6–3.4 THz was scanned in steps of 1 GHz. Nearly all predicted absorption lines are present in the measured signal.

A closer analysis of the results shows that the noise current is only slightly increasing toward thicker InGaAs layer and  $\sim 15 \text{ pA}/(\text{Hz}^{-1/2})$  for all receiver structures. Thus, the improvement of the SNR is mainly due to the increase of the generated photocurrent, i.e., the higher conversion efficiency of the modified receiver. Since the responsivity enhancement (factor 6.5) is equivalent to a 16 dB rise of the signal, the main effect of the 20 dB performance improvement can be assigned to the increased absorption volume.

The superior SNR of the realized system is essential for industrial applications, where fast acquisition times are required. Assuming the well-known square root dependence of noise and filter bandwidth, the SNR will decrease

by about 23 dB if the integration time is reduced from 200 to 1 ms (filter slope 12 dB/octave). Hence, the implemented system will still provide more than 45 dB SNR at 1 THz and a bandwidth of 2.8 THz at such short integration times.

In summary, the increase of the InGaAs layer thickness in InGaAs/InAlAs photoconductive receivers improves the SNR of 1.5  $\mu\text{m}$  cw THz systems by about 20 dB and extends the system bandwidth by about 50%. Applied to a coherent cw THz system, a SNR of 70 dB at 1 THz and a bandwidth of more than 3.5 THz were achieved. These results are the best performance reported in literature and are therefore superior to any 800 nm photomixing system. Future investigation will show if the performance can be further enhanced by other variations or combinations of the layer thicknesses of the InGaAs/InAlAs heterostructure.

## References

1. F. Ellrich, T. Weinland, D. Molter, J. Jönuscheit, and R. Beigang, *Rev. Sci. Instrum.* **82**, 053102 (2011).
2. A. Roggenbuck, K. Thirunavukkuarasu, H. Schmitz, J. Marx, A. Deninger, I. C. Mayorga, R. Güsten, J. Hemberger, and M. Grüninger, *J. Opt. Soc. Am. B* **29**, 614 (2012).
3. N. Kim, S.-P. Han, H. Ko, Y. A. Leem, H.-C. Ryu, C. W. Lee, D. Lee, M. Y. Jeon, S. K. Noh, and K. H. Park, *Opt. Express* **19**, 15397 (2011).
4. H. Roehle, R. J. B. Dietz, H.-J. Hensel, J. Böttcher, H. Künzel, D. Stanze, M. Schell, and B. Sartorius, *Opt. Express* **18**, 2296 (2010).
5. J. Sigmund, C. Sydlo, H. L. Hartnagel, N. Benker, H. Fuess, F. Rtz, T. Kleine-Ostmann, and M. Koch, *Appl. Phys. Lett.* **87**, 252103 (2005).
6. L. Fekete, H. Nemec, Z. Mics, F. Kadlec, P. Kuzel, V. Novak, J. Lorincik, M. Martin, J. Mangeney, J. C. Delagnes, and P. Mounaix, *J. Appl. Phys.* **111**, 093721 (2012).
7. S. Hisatake, G. Kitahara, K. Ajito, Y. Fukada, N. Yoshimoto, and T. Nagatsuma, *IEEE Sens. J.* **13**, 31 (2013).
8. D. Stanze, A. Deninger, A. Roggenbuck, S. Schindler, M. Schlak, and B. Sartorius, *J. Infrared Millim. Terahz. W.* **32**, 225 (2011).
9. D. Stanze, T. Göbel, R. J. B. Dietz, B. Sartorius, and M. Schell, *Eletron. Lett.* **47**, 1292 (2011).
10. A. Roggenbuck, H. Schmitz, A. Deninger, I. Cámara Mayorga, J. Hemberger, R. Güsten, and M. Grüninger, *New J. Phys.* **12**, 043017 (2010).